IOT4AG AGRICULTURAL LEAF AND SOIL SENSORS

Cherie R. Kagan[1,2,3], Roy H. Olsson[1*], and Kevin T. Turner[2,4*]*
[1]Department of Electrical & Systems Engineering, University of Pennsylvania, Philadelphia, Pennsylvania, USA
[2]Department of Materials Science & Engineering, University of Pennsylvania, Philadelphia, Pennsylvania, USA
[3]Department of Chemistry, University of Pennsylvania, Philadelphia, Pennsylvania, USA
[4]Department of Mechanical Engineering & Applied Mechanics, University of Pennsylvania, Philadelphia, Pennsylvania, USA

ABSTRACT

IoT4Ag is the short name for the US NSF Engineering Research Center for the Internet of Things for Precision Agriculture. The Center's mission is "to create and translate to practice Internet of Things (IoT) technologies for precision agriculture and to train and educate a diverse workforce that will address the societal grand challenge of food, energy, and water security for decades to come." To deliver on this mission, one aspect of the Center's research is to create application-specific, multi-mode, low-cost, highly-distributable leaf and soil sensors to monitor plant and soil health at the farm scale. Here, we describe the design, fabrication, and characterization of zero-power optical leaf and radio frequency (RF) soil sensors composed of biocompatible and biodegradable materials and manufactured using large-area, low-cost fabrication technologies to make visible the invisible targets that affect plant health.

KEYWORDS

optical sensors, RF sensors, agriculture, leaf sensors, soil sensors, imprinting, printing, biodegradable, biocompatible

INTRODUCTION

IoT4Ag, the US NSF Engineering Research Center for the Internet of Things for Precision Agriculture, was launched in 2020 [1]. The Center's work aims to address the societal grant challenge of food, energy, and water security, which in the face of a growing population; the negative impacts of climate change and agrochemical use on our environment; and the competition for arable land, energy, and water resources, calls for an increase in food production and yet a decrease in land, water, energy, and agrochemical use. Farm management requires monitoring of agricultural crops. Today, monitoring is still accomplished primarily through the expensive, labor-intensive, and time-consuming process of crop scouting, by manual sampling and documenting the state of the field. Precision agriculture involves the use of technology to acquire and analyze data from the field. However, current technologies such as sensors are limited or non-existent to spatially-, temporally-, and compositionally-monitor the state of the field, data is coarse-grained and siloed in equipment, communications infrastructure is limited or non-existent in the rural environments typical of farms, and interventions are often reactive and over-provisioned, and thus increase the economic and environmental costs of farming.

IoT4Ag is responding by creating integrated sensor-communication-response systems, spanning hardware to software, that capture the microclimate and spatially-, temporally-, and compositionally-map heterogeneous stresses so farmers can predict and efficiently control the state of the farm. The Center is driven by the agricultural-specific use case of IoT technologies, i.e., by the need to develop technologies and integrated systems that meet the scale, environment, practices, and socioeconomic constraints of farming. Here, we describe leaf and soil sensor platforms designed to monitor targets that cannot be observed directly, e.g., abiotic and biotic stresses such as water, nutrients, volatile organic compounds, toxins, and pathogens. The sensor designs are constrained to meet the needs for low-cost and large-scale manufacturing, for deployment consistent with existing farming practices, and to be biocompatible/biodegradable so large numbers of sensors can be deployed and "forgotten", i.e., not later retrieved from the field.

Optical Leaf Sensors

Current leaf sensors, such as leaf moisture sensors, typically require a power source and are large and expensive. Some sensors aren't even placed on the leaves, and therefore don't measure the leaves directly. With the growing use of remote imaging technologies in agriculture, such as cameras mounted on farm machinery or on agricultural robots, there is an opportunity to introduce optical sensors that adhere to leaves and monitor target measurands directly, such as leaf transpiration, temperature, volatile organic compounds, and toxins, which are indicators of plant stress.

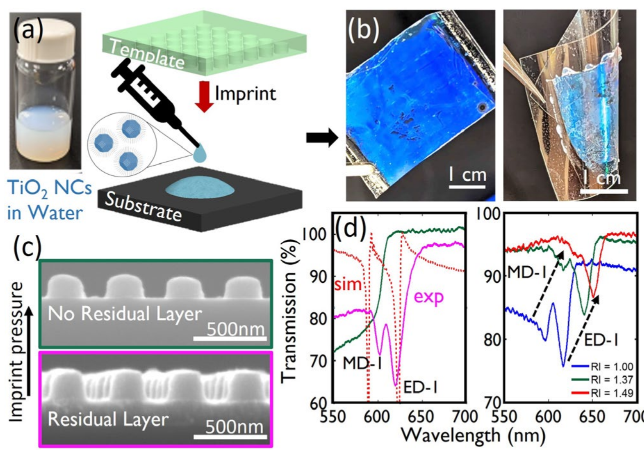

Figure 1: (a) Photograph of an aqueous, TiO_2 nanocrystal (NC) dispersion and schematic of the process of direct imprinting into the NC dispersion to (b) create, as shown in photographs, large-area dielectric metasurfaces on glass (left) and polymeric (right) substrates. (c) Control over the imprint pressure is used, as shown in scanning electron microscopy (SEM) images, to create metasurfaces composed of two-dimensional NC pillar arrays without (green) and with (pink) a residual NC layer. (d) Left, transmittance spectra of metasurfaces without (green) and with (pink) a residual NC layer (experimental) and with a residual layer (red, simulation). Right, experimental transmittance spectra of a NC metasurface as a function of the refractive index of the surrounding environment.

IoT4Ag is designing colorimetric leaf sensors by integrating optical metasurfaces with adaptive polymers that change color as the dielectric constant or geometry of the polymer changes in response to target measurands [2], [3]. The metasurfaces advantageously do not bleach in sunlight, like sensors based on light absorption and emission. The optical metasurfaces are highly reflective, requiring no power sources, with colors (i.e., operating wavelength ranges) and quality factors (Q) that are tailored by selection of the material composition and the size, shape, and arrangement of dielectric or metallic nanostructures [4], [5]. The sensors are designed to be detected using visible to near-infrared, multispectral, and/or hyperspectral cameras. The sensors must also be fabricated using biocompatible and biodegradable materials to deploy and forget; be flexible and structured to contact leaf surfaces; and be manufactured using low-cost and large-area techniques to meet the need for large numbers of devices to monitor crops at field scale.

To realize these sensors, we developed direct imprinting of colloidal nanocrystal (NC) inks [6], [7]. Recently, we reported a room temperature, environmentally-benign, water-based, single-step direct nanoimprinting process using colloidal TiO_2 nanocrystal (NC) inks (Fig. 1a) to create large-area optical metasurfaces on rigid and flexible polymer substrates (Fig. 1b) [8]. TiO_2 is selected for its biocompatibility, high refractive index, and low loss. The TiO_2 NC inks are free of polymer additives, so the patterned structures have a high refractive index of 1.94 ± 0.02 at 543 nm. A master nanoimprint template is structured to form metasurfaces with two-dimensional nanopillar gratings. By controlling the imprint pressure, the process can be tailored to deposit only nanopillar arrays or to additionally leave a residual NC underlayer (Fig. 1c). Optical transmission spectra of metasurfaces without (green) and with (pink) a residual underlayer are shown in Figure 1d. For the NC pillar arrays without the residual layer, Mie resonances are not observed as the optical path length (i.e., the product of the refractive index and the height of the pillars) is too small. For the NC pillar arrays with the residual layer, the residual layer acts as a waveguide. Guided mode resonances within the waveguide couple to the overlaying nanopillar gratings and scatter into free space, forming high-Q, quasi-guided modes (QGMs) [9], [10], as seen by first-order magnetic dipole resonances (MD-1) and electric dipole (ED-1) resonances, also consistent with simulations. The wavelength of the MD and ED resonances depend on the guided mode resonances and therefore the thickness of the NC waveguide, but negligibly on the height of the nanopillar grating.

The wavelengths of the QGM resonances depend strongly on the refractive index of the environment. Figure 1e shows the transmission spectra for a metasurface as the environment refractive index is tuned from 1.00 (air) to 1.49 (toluene) by depositing different solvents on the sample surface. The MD-1 and ED-1 resonances redshift consistent with a sensitivity (S) of 70.4 and 69.1 nm/RIU, respectively, where RIU is the refractive index unit. The amplitude of the resonances decreases as the refractive index contrast between the metasurface and the environment decreases. Interestingly, these values for S are advantageously larger than those fabricated from a bulk TiO_2 waveguide, consistent with simulations showing the weaker confinement of the electric and magnetic fields within the NC waveguides and greater extension into the environment due to their lower refractive index. To realize good sensors, devices with sharp resonances that show greater spectral shifts are advantageous and thus the sensing capability of the devices can be described by a figure of merit $FOM = Q \times S$. The FOM for the ED-1 and MD-1 resonances are 4082 and 3325, respectively. These TiO_2 NC dielectric metasurfaces serve as a platform for the scalable manufacturing of biocompatible/biodegradable, flexible optical sensors integrated with different adaptive polymers to probe target measurands directly on the leaves of crops.

RF Soil Sensors

Current soil sensors, such as soil moisture sensors, typically require a power source and are large and expensive to deploy and maintain. Thus, these sensors are currently deployed in small numbers, and therefore, decisions in farming practices rely on sparsely collected data from sensors distributed at a handful of different locations across large agricultural fields. The growth in IoT technologies opens opportunities for high spatial and temporal monitoring of targets in the soil, such as soil moisture, nutrients, and pathogens.

IoT4Ag is designing RF soil sensor nodes, composed of antennas, acoustic resonators, and capacitive sensors, that are low cost, passive, wireless, and mostly biodegradable [11], [12], [13]. The sensor nodes are designed to operate in the 902-928 MHz industrial, scientific, and medical (ISM) band to allow signals to penetrate into/out of the soil, while also requiring relatively small antennas. An RF transceiver at a base station is used to transmit a chirp, i.e., a multi-frequency signal, that is received by the sensor node antenna. The signal excites the acoustic resonator, driving it to vibrate strongly and store RF energy in the mechanical vibrations of the resonator. The resonator is designed to have high Q, allowing energy to be stored long enough for ambient reflections of the chirp to dissipate. The resonator releases the stored energy with a time delay at its resonant frequency (f_o), which is transmitted by the sensor antenna and received by the base station. f_o of the resonator depends on the capacitance of the sensor and thus on the properties of the soil, allowing sensors to be designed to measure targets of interest.

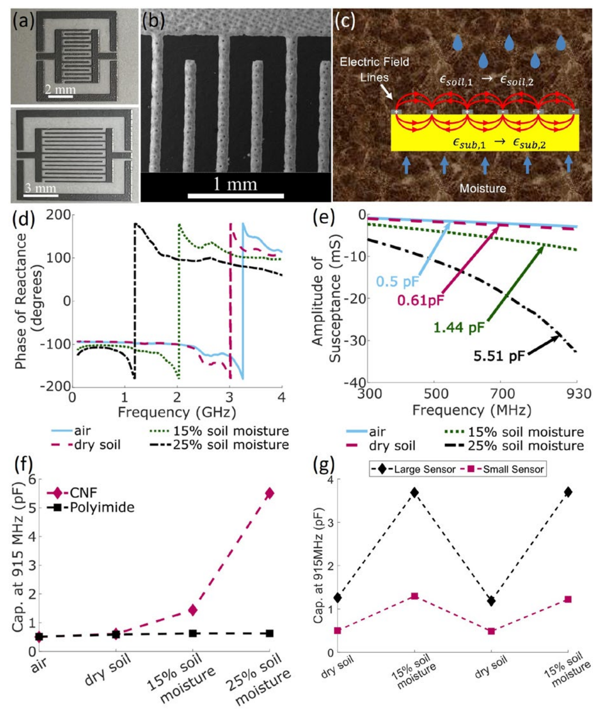

Figure 2: (a) Photographs and (b) SEM image of soil moisture sensors fabricated by screen printing Ag inks on CNF-infused cardstock. (c) Schematic of sensor operation as capacitance changes as the dielectric constant of the soil (ε_{soil}) and substrate (ε_{sub}) are altered in response to variations in soil moisture. (d) Phase of reactance and (e) amplitude of susceptance as a function of frequency for sensors in air, dry soil, and wet soil for the small sensor in (a). Equivalent capacitance at 915 MHz for (f) for sensors fabricated on CNF-infused cardstock and polyimide substrates as a function of soil moisture and (g) small and large sensors fabricated on CNF-infused cardstock over two measurement cycles of dry to wet soil.

To achieve sensor nodes that meet the agricultural-specific use case, the largest components of the nodes, i.e., the substrate, the sensor, and the antenna must be selected from materials that are biodegradable and that can be fabricated using low-cost techniques. Polymer substrates, such as Kapton and polyethylene terephthalate, commonly used in flexible electronics are not biodegradable. Paper substrates are biodegradable, but their fibrous structure makes them rough and highly porous, and thus, it is difficult to fabricate electrically conductive wires and antennas. Specialty papers, with fillers, improve surface properties but typically include non-biodegradable polymers. Recently nanocellulose-based nanofibrils (CNFs) have been explored as moisture sensing materials [14], [15], [16], but they have limited mechanical stability under varying humidity conditions.

We developed a fully biodegradable CNF-infiltrated cardstock composite to use as a substrate for agricultural moisture sensors [12], [13]. An aqueous CNF gel is coated on wet cardstock, allowed to infuse for ~1.5 h, and then a second layer is applied. Samples are heat pressed at 60 ˚C for 20 min and then oven dried at 60 ˚C for 12 h to drive off residual water. The CNF-composite has a rms roughness of 0.52 μm, similar to that of 0.47 μm for polyimide substrates and an order of magnitude smaller than the 3.5 μm roughness of the cardstock alone. We fabricate high-quality electrical structures from commercial, Ag nanoflake inks using a low-cost, large-area screen-printing process. Figures 1a,b show images of interdigitated, capacitive moisture sensors. Traces are printed on the CNF-composite substrates, and yield structures with average heights of 13 ± 2.6 μm, similar to that of 14 ± 1.1 μm for traces fabricated on polyimide substrates.

The capacitive sensor design, i.e., the number of fingers and their length and spacing is selected so that the electrode spacing is larger than the substrate thickness, so field lines travel through the moisture-responsive CNF-composite substrate (Fig. 2c); and to limit the equivalent inductance (L_s), created by current flow through the sensor fingers, and the sensor capacitance (C), and thus to obtain self-resonances at frequencies $f_o = \frac{1}{2\pi\sqrt{L_s C}}$ in excess of the 902-928 MHz ISM band. Above f_o, the sensor impedance is dominated by the inductance and the sensor no longer behaves as a capacitor. The sensor Q-factor describes the energy stored by the capacitor with respect to energy dissipated by thermal loss, where $Q = \frac{1}{2\pi f C R_s}$ and R_s is the equivalent series resistance caused by loss in the fingers. To achieve large f_o and Q, small sensor C is advantageous, but it is limited by the electrode spacing. For sensors with the same C, smaller sensors with lower L_s and R_s yield larger f_o and Q. Two ground planes are added, one on each side of the sensor, to allow RF measurements using ground-signal-ground probes.

The RF soil sensors are responsive to changes in soil moisture because the dielectric constant of the hygroscopic, CNF-composite substrate (ε_{sub}) and that of the soil (ε_{soil}) increase with greater soil water content (Fig. 2c). We measured the sensors' admittance as a function of frequency. The higher ε_{sub} and ε_{soil} as soil moisture increases, decreases f_o, requiring the sensor design to have a large enough f_o when operating in wet soil. In Figure 2d, f_o is seen as the frequency at which the sign of the phase switches from negative to positive. The small sensor f_o remains above 928 MHz for all soil moisture conditions. The amplitude of sensor susceptance, the imaginary part of admittance, is shown at capacitive sensor operation frequencies <930 MHz and becomes more negative as the sensor capacitance increases as soil moisture increases. Figure 2f shows the capacitance at 915 MHz for sensors fabricated on moisture-sensitive CNF-composite substrates, in comparison to those fabricated on polyimide. The polyimide sensors respond only to changes in ε_{soil}, but the moisture sensitivity of the CNF-composite substrates also creates a change in ε_{sub}, and thus advantageously a large modulation in sensor capacitance with soil moisture. These sensors are robust to cycling of soil moisture levels (Fig. 2g).

While Ag and Au NC inks are well-studied and available commercially, Ag is not biocompatible/biodegradable and Au is costly. These inks also typically require post-deposition annealing at temperatures >120 ˚C or high-intensity laser irradiation to decompose ink additives [17], [18], introduced to stabilize the NCs in solvents and control ink viscosity, and to drive sintering to achieve high conductivity traces. Cu NC inks stand out as low-cost, biodegradable/biocompatible materials that can be used to fabricate electrical conductors [19], [20]. To fabricate fully biodegradable devices at low cost for RF soil sensors, we developed colloidal Cu NC inks and a room temperature, chemically-driven sintering process, using non-corrosive chemical treatments compatible with fabrication on polymer and paper substrates [21]. The process stabilizes the Cu NC-based materials toward oxidation and yields high-conductivity Cu traces for sensors and antennas.

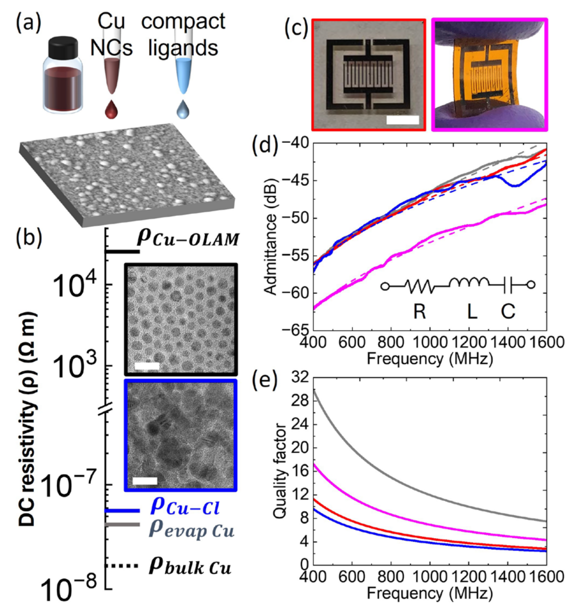

Figure 3: (a) Process schematic and SEM image of a highly conductive Cu film fabricated by solution-deposition of oleylamine (OLAM)-capped Cu NC inks followed by surface treatment using compact ligands, that exchange the OLAM ligands and drive NC sintering at room temperature. (b) Resistivity (ρ), benchmarked against evaporated Cu films and bulk Cu, and transmission electron microscopy (TEM) images of 4.5 nm diameter OLAM-capped Cu NC films before (black) and after (blue) ligand exchange with NH_4Cl. Scale bar: 10 nm. (c) Photographs of capacitive sensors fabricated from Cu NC inks on glass (left) and Kapton (right). Scale bar: 3 mm. (d) Measured (solid lines) and equivalent circuit model fit (dashed lines) of admittance and (e) calculated Q-factor for an evaporated Cu film (grey) and samples fabricated by spin coating (red) and doctor-blade coating (blue) NC inks on glass, and by spin-coating NC inks on Kapton (magenta).

Colloidal Cu NC samples are synthesized using wet-chemical methods and tailored in size (e.g., to be 4.5 nm or 15 nm diameter) by controlling the concentration of oleylamine (OLAM) ligands introduced in the reaction flask. The Cu NC synthesis and handling post synthesis are carried out under an inert atmosphere. The OLAM ligands stabilize the NCs as dispersions in solvents to form inks (Fig.

3a). The NC inks are deposited on rigid and flexible substrates to form 10s of nm to micron scale thick films by spin coating or doctor-blade coating.

The long-chain organic, OLAM ligands maintain a separation between the Cu NCs, as seen in transmission electron microscopy (TEM) images (Fig. 3b). The intervening OLAM ligands act as barriers to charge transport and yield films with high DC resistivity ($\rho_{Cu-OLAM}$) $> 10^4$ Ω·m. We treat the OLAM-capped NC films at room temperature with methanolic solutions of compact ligands (Fig. 2a), such as environmentally-benign, non-corrosive, and low-cost thiocyanate (SCN^-) and chloride (Cl^-), introduced from their ammonium salts [7], [22]. Exchange of OLAM-capped NC films with these short inorganic ions triggers NC fusion and grain growth to form conductive pathways, as exemplified in Figure 2b by the TEM image and the ~10^{12} smaller $\rho_{Cu-Cl} = 5.45 \times 10^{-8}$ Ω·m for Cl^--treated Cu NC films, approaching the resistivity of evaporated Cu films $(\rho_{Cu-evap})$ and within a factor of 3.2 of that for bulk Cu ($\rho_{Cu-bulk}$). Cl^--treated, 4.5 nm diameter Cu NC films yield films with the largest grain size and lowest DC resistivity. Cl^- more effectively removes OLAM ligands and SCN^- forms stronger bonds to Cu limiting NC sintering. The larger surface-to-volume ratio and chemical potential of smaller NCs provides a greater thermodynamic driving force for NC sintering. The SCN^- and Cl^- treated and thus sintered NC films also remain air stable for months, limited to oxidation of the top surface of the film.

We demonstrate the use of such Cu NC inks and the chemically-driven, room temperature sintering of their films to create RF capacitive devices on glass and polyimide substrates (Fig. 3c). In our first demonstration, we use photolithography to pattern the films into micron-scale interdigitated capacitors with structures like those we fabricated from Ag inks. All devices are fabricated by spin or doctor-blade coating of 4.5 nm diameter Cu NCs and Cl^- ligand exchange to achieve the lowest DC resistivity. For all devices studied here, the calculated f_0 values exceed 2 GHz. Frequency-dependent admittance measurements (Fig. 3d) and fits to the equivalent circuit model yield capacitances of ~0.6 pF for Cu NC devices fabricated by spin coating or doctor-blade coating, which are similar to those for evaporated Cu devices. The capacitance of Cu NC devices fabricated on polyimide substrates is lower than those on glass since the dielectric constant of the polymer substrate is smaller. The higher ρ of Cu NC films compared to evaporated Cu films yields devices with a 3x higher R_s and thus lower Q. Notably, and advantageously for our RF sensor design on low dielectric constant substrates, capacitors fabricated on polymer substrates have the highest Q.

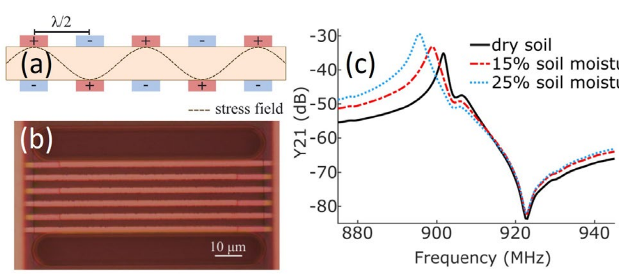

Figure 4: (a) Schematic and (b) optical image of a double-patterned Lamb-wave resonator (LWR) composed of $Al_{0.7}Sc_{0.3}N$. (c) Admittance of a LWR-sensor node in loamy sand measured at three different soil moisture levels.

One component of the sensor node is the tank circuit that serves as a resonator, with a frequency that is modulated by the sensor capacitance and establishes the signal of interest. Chip-based radio-frequency identification (RFID) methods rely on tuning of resonant antennas, which have low Q of ~100, limiting communication ranges to ~10 m in air, and small changes in capacitance often pull the node out of the 902 – 928 MHz ISM band [23], [24], [25]. Chipless RFID, passive wireless sensor nodes have been reported at 2.4 GHz using RF cavities with a Q of 1000 and interrogation ranges of ~40 m, but they are prohibitively large ($\approx 706\ cm^3$) [26].

IoT4Ag is constructing acoustic wave resonators to achieve small ($< 0.5\ mm^3$) devices with high Q operating in the 902 – 928 MHz ISM band [11]. We designed a Lamb-wave resonator (LWR) composed of double-patterned (top and bottom) interdigitated electrodes (Fig. 4a,b). The interdigitated electrodes launch an acoustic wave into a resonant structure, depicted by the stress field, which has an acoustic velocity (measured as a change in f_o) that depends on changes in the measurand. The LWR stores the RF interrogation signal at f_o before reconverting to an electrical signal. To use acoustic resonators to measure frequency shifts at long range, the $FOM = Q \times k_t^2$ where k_t^2 is the electromechanical coupling coefficient of the resonator. We use a 380 nm thick $Al_{0.7}Sc_{0.3}N$ layer, a relatively new piezoelectric material with enhanced k_t^2, and AlCu electrodes, which provide low resistance contacts and have a small Young's modulus for good k_t^2. The device has f_o of 894.42 MHz, Q of 900, and k_t^2 of 7.9%, and thus a FOM of 71.53, which is 37.5% larger than the FOM of a state-of-the-art LWR at the closest frequency ($f_o = 801.4\ MHz, FOM = 52$). f_o is just below the 902 MHz band and can be adjusted by decreasing the pitch of the LWR electrodes.

The LWR is integrated with a soil moisture sensor, like those in Figure 2, using the Keysight Advanced Design System. The measured sensor responses are connected in series with the measured LWR. The frequency dependent admittance (Y_{21}) of the LWR-sensor node is shown in Figure 4c for loamy sand soil that is dry and with 15% and 25% moisture. A 25% increase in soil moisture shifted f_o by 6.21 MHz, well larger than the minimum detectable frequency of 64 kHz of the node or equivalently of a 0.5% change in soil moisture.

CONCLUSION

Optical leaf and RF soil sensor nodes are being realized to deliver IoT technologies for the application-specific use case of agriculture, which require biocompatible/biodegradable devices that are fabricated using low-cost, scalable, and low-temperature manufacturing processes. The sensor designs establish platforms for optical and RF sensors, where adaptive materials responsive to target measurands, can provide specificity to monitor targets that cannot be observed directly, such as water, nutrients, volatile organic compounds, toxins, and pathogens that are indicators of plant stress. In IoT4Ag, these sensors are one leg of integrated sensor-communication-response systems being developed for use in farming of tree and row crops to meet the societal challenge of advancing technology to improve food, energy, and water security. The technologies being developed here have broad applications beyond the agricultural sector.

ACKNOWLEDGEMENTS

We are grateful for the hard work and creativity of the students and postdoctoral fellows who performed the research: Gokulanand M. Iyer, Chavez F. K. Lawrence, Akhila Mallavarapu, Jun Xu, Anne-Marie Zaccarin, and Tianshuo Zhao. This work is primarily supported by the IoT4Ag Engineering Research Center funded by the National Science Foundation (NSF) under NSF Award Number EEC-1941529. This work was carried out in part at the Singh Cetner for Nanotechnology, part of the National Nanotechnology

Coordinated Infrastructure Program, which is supported under NSF award NNCI-2025608.

REFERENCES

[1] C. R. Kagan, D. P. Arnold, D. J. Cappelleri, C. M. Keske, and K. T. Turner, "Special report: The Internet of Things for Precision Agriculture (IoT4Ag)," *Comput Electron Agric*, 196, (2022).

[2] C. R. Kagan, D. P. Arnold, M. G. Allen, and R. H. Olsson, "IoT4Ag: MEMS-Enabled Distributed Sensing, Communications, and Information Systems for the Internet of Things for Precision Agriculture," in *Proceedings of the IEEE International Conference on Micro Electro Mechanical Systems (MEMS)*, Institute of Electrical and Electronics Engineers Inc., Jan. 2021, pp. 350–353.

[3] W. Chen *et al.*, "Angle-Independent Optical Moisture Sensors Based on Hydrogel-Coated Plasmonic Lattice Arrays," *ACS Appl Nano Mater*, 1, 1430–1437, (2018).

[4] A. I. Kuznetsov *et al.*, "Roadmap for Optical Metasurfaces," *ACS Photonics*, 11, 816–865, (2024).

[5] K. Koshelev and Y. Kivshar, "Dielectric Resonant Metaphotonics," *ACS Photonics*, 8, 102–112, (2020).

[6] Y. Cai, Y. C. Choi, and C. R. Kagan, "Chemical and Physical Properties of Photonic Noble-Metal Nanomaterials," *Advanced Materials*, 35, (2023).

[7] A. T. Fafarman *et al.*, "Chemically Tailored Dielectric-to-Metal Transition for the Design of Metamaterials from Nanoimprinted Colloidal Nanocrystals.," *Nano Lett*, 13, 350–7, (2013).

[8] A. Mallavarapu, C. FK. Lawrence, B. Huang, B. O. Torres Maldonado, P. Arratia, and C. R. Kagan, "TiO2 Metasurfaces with Visible Quasi-Guided Mode Resonances via Direct Imprinting of Aqueous Nanocrystal Dispersions," *ACS Appl Nano Mater*, 6, 17294–17300, (2023).

[9] R. Magnusson and S. S. Wang, "Theory and applications of guided-mode resonance filters," *Applied Optics,* 32, 2606–2613, (1993).

[10] A. Szeghalmi, E. Bernhard Kley, and M. Knez, "Theoretical and Experimental Analysis of the Sensitivity of Guided Mode Resonance Sensors," *The Journal of Physical Chemistry C*, 114, 21150–21157, (2010).

[11] A.-M. Zaccarin, G. M. Iyer, A. Kochhar, R. Vetury, K. T. Turner, and R. H. Olsson, "High Performance Lamb Wave Resonator Operating in the 900 MHz ISM Band for Wireless Sensing Applications," in *2023 IEEE/MTT-S International Microwave Symposium - IMS 2023*, IEEE, (2023), pp. 1168–1171.

[12] G. M. Iyer, A.-M. Zaccarin, R. H. Olsson, and K. T. Turner, "Fabrication and Characterization of Cellulose-Based Materials for Biodegradable Soil Moisture Sensors," in *2022 IEEE Sensors*, IEEE, (2022), pp. 1–4.

[13] A.-M. Zaccarin, G. M. Iyer, R. H. Olsson, and K. T. Turner, "Fabrication and Characterization of Soil Moisture Sensors on a Biodegradable, Cellulose-Based Substrate," *IEEE Sens J*, 24, 7235–7243, (2024).

[14] T. Syrový *et al.*, "Wide range humidity sensors printed on biocomposite films of cellulose nanofibril and poly(ethylene glycol)," *J Appl Polym Sci*, 136, (2019).

[15] G. Ayissi Eyebe, B. Bideau, N. Boubekeur, É. Loranger, and F. Domingue, "Environmentally-friendly cellulose nanofibre sheets for humidity sensing in microwave frequencies," *Sens Actuators B Chem*, 245, 484–492, (2017).

[16] A. Rivadeneyra *et al.*, "Cellulose nanofibers as substrate for flexible and biodegradable moisture sensors," *Compos Sci Technol*, 208, 108738, (2021).

[17] Y. Zhang *et al.*, "Facile Preparation of Monodisperse, Impurity-Free, and Antioxidation Copper Nanoparticles on a Large Scale for Application in Conductive Ink," *ACS Appl Mater Interfaces*, 6, 560–567, (2014).

[18] V. Abhinav K, V. K. Rao R, P. S. Karthik, and S. P. Singh, "Copper conductive inks: synthesis and utilization in flexible electronics," *RSC Adv*, 5, 63985–64030, (2015).

[19] Z. Li, S. Chang, S. Khuje, and S. Ren, "Recent Advancement of Emerging Nano Copper-Based Printable Flexible Hybrid Electronics," *ACS Nano*, 15, 6211–6232, (2021).

[20] X. Dai, T. Zhang, H. Shi, Y. Zhang, and T. Wang, "Reactive Sintering of Cu Nanoparticles at Ambient Conditions for Printed Electronics," *ACS Omega*, 5, 13416–13423, (2020).

[21] J. Xu *et al.*, "Chemically-Driven Sintering of Colloidal Cu Nanocrystals for Multi-scale Electronic and Optical Devices" (2024).

[22] A. T. Fafarman *et al.*, "Air-stable, nanostructured electronic and plasmonic materials from solution-processable, silver nanocrystal building blocks.," *ACS Nano*, 8, 2746–54, (2014).

[23] S. Kim, Y. Kawahara, A. Georgiadis, A. Collado, and M. M. Tentzeris, "Low-Cost Inkjet-Printed Fully Passive RFID Tags for Calibration-Free Capacitive/Haptic Sensor Applications," *IEEE Sens J*, 15, 3135–3145, (2015).

[24] C. Boyer and S. Roy, "— Invited Paper — Backscatter Communication and RFID: Coding, Energy, and MIMO Analysis," *IEEE Transactions on Communications*, 62, 770–785, (2014)..

[25] F. Fuschini, C. Piersanti, F. Paolazzi, and G. Falciasecca, "Analytical Approach to the Backscattering from UHF RFID Transponder," *IEEE Antennas Wirel Propag Lett*, 7, 33–35, (2008).

[26] D. J. Thomson, D. Card, and G. E. Bridges, "RF Cavity Passive Wireless Sensors With Time-Domain Gating-Based Interrogation for SHM of Civil Structures," *IEEE Sens J*, 9, 1430–1438, (2009).

CONTACT

*C. R. Kagan, tel: +1-215-573-4384; kagan@seas.upenn.edu
R. H. Olsson, tel: +1-215-898-6426; rolsson@seas.upenn.edu
K.T. Turner, tel: +1-215-573-7485; ktturner@seas.upenn.edu